

PRETVM: Predictable, Efficient Virtual Machine for Real-Time Concurrency

Shaokai Lin
UC Berkeley
Berkeley, USA

Erling Jellum
NTNU
Trondheim, Norway

Mirco Theile
TU Munich
Munich, Germany

Tassilo Tanneberger
TU Dresden
Dresden, Germany

Binqi Sun
TU Munich
Munich, Germany

Chadlia Jerad
University of Manouba
Manouba, Tunisia

Ruomu Xu
UC Berkeley
Berkeley, USA

Guangyu Feng
UC Berkeley
Berkeley, USA

Christian Menard
TU Dresden
Dresden, Germany

Marten Lohstroh
UC Berkeley
Berkeley, USA

Jeronimo Castrillon
TU Dresden
Dresden, Germany

Sanjit Seshia
UC Berkeley
Berkeley, USA

Edward Lee
UC Berkeley
Berkeley, USA

Abstract—This paper introduces the Precision-Timed Virtual Machine (PRETVM), an intermediate platform facilitating the execution of quasi-static schedules compiled from a subset of programs written in the Lingua Franca (LF) coordination language. The subset consists of those programs that in principle should have statically verifiable and predictable timing behavior. The PRETVM provides a schedule with well-defined worst-case timing bounds. The PRETVM provides a clean separation between application logic and coordination logic, yielding more analyzable program executions. Experiments compare the PRETVM against the default (more dynamic) LF scheduler and show that it delivers time-accurate deterministic execution.

Index Terms—Cyber-Physical Systems, Real-Time Systems, DAG Scheduling, Virtual Machine, Concurrency

I. INTRODUCTION

When developing real-time software for Cyber-Physical Systems (CPSs), the conventional strategy often adopts a bottom-up approach, where the emphasis is first placed on defining the “how”—for instance, using a preemptive EDF scheduler—in hopes of realizing the “what”, i.e., the desired timing behavior. This bottom-up process relies heavily on experimental feedback to find out whether a system is able to meet system-level timing constraints. Iteratively, code optimizations are carried out until the desired behavior is achieved. Yet, the bottom-up method complicates code validation and upgrades, and it renders implementations platform-specific and only works well in systems where multiple runs of the same code yield very similar timing behavior. Code obtained

The work in this paper was supported in part by the National Science Foundation (NSF), award #CNS-2233769 (Consistency vs. Availability in Cyber-Physical Systems), by DARPA grant FA8750-20-C-0156, by Intel, and by the iCyPhy Research Center (Industrial Cyber-Physical Systems), supported by Denso, Siemens, and Toyota. This work was also supported, in part, by the German Federal Ministry of Education and Research (BMBF) as part of the program “Souverän. Digital. Vernetzt.”, joint project 6G-life (16KISK001K), and by the German Research Council (DFG) through the InterMCore project (505744711). Mirco Theile and Binqi Sun were supported by the Chair for Cyber-Physical Systems in Production Engineering at TUM.

through such a process, therefore, tends to not be useable on different platforms and is challenging to prove safe. As Cyber-Physical Systems become more software-defined (e.g., in the automotive industry [1]) and increasingly often implemented using multi-core and heterogeneous hardware, the bottom-up approach becomes less feasible and attractive.

Henzinger and Kirsch [2] observe that a lot of these difficulties are due to an entanglement of concerns between “reactivity,” which refers to real-time interaction with a physical environment, “schedulability,” which concerns real-time execution in a specific execution environment, and “functionality,” such as control laws and device drivers. The Giotto language and methodology they developed, which introduced the concept of Logical Execution Time (LET), meant specifically to help programmers separate these concerns. A Giotto program explicitly specifies the exact real-time interaction of software components with the physical world, leaving it to the Giotto compiler (not the software or control engineer) to generate timing code that ensures the specified timing behavior on a given platform. The timing code, known as E code, encodes Giotto’s LET semantics and runs on the Embedded Machine, a virtual machine that makes E code portable [3].

The recently emerged Lingua Franca (LF) [4], [5] coordination language and its underlying reactor model [6] can be characterized as a generalization of Giotto and LET [7]. It takes the separation between reactivity and schedulability a step further by decoupling the passage of physical time from logical time, except when interactions with the physical world are involved (through timers, sensors, and actuators) [8]. In part because LF is not strictly task-based and allows sporadic events, the scheduling of LF programs is carried out dynamically, at runtime. While the timing behavior is specified in the LF code, alignment with physical time is best-effort and without hard guarantees that could be derived based on a quasi-static schedule.

This paper describes an augmentation of the LF toolchain

that generates quasi-static schedules. We do this through a compiler extension, runtime integration, and virtual machine abstraction called the **Precision-Timed Virtual Machine**, or in short, PRETVM. The functionality that PRETVM offers to LF is similar to what the E Machine [3] provides for LET. PRETVM enables a methodology for obtaining predetermined temporal behavior for the subset of LF programs comprising sequences of periodic task sets. Based on a directed acyclic graph (DAG) representation of the program, a **partitioned quasi-static schedule** can be derived using different schedulers. This quasi-static schedule, after being translated into our PRETVM bytecode for each partition, can be executed using multiple worker threads. We show that our approach exhibits predictable timing and can leverage existing work in multi-core mapping and scheduling, such as Edge Generation Scheduling for DAG Tasks [9].

In this work, we focus on a subset of LF programs whose behavior can be statically analyzed by our approach. We exclude “dynamic” features of LF, such as actions and physical connections, and save them for future work.

Contributions: In this paper, we present the following key contributions:

- 1) We present the Precision-Timed Virtual Machine, PRETVM, as an intermediary platform supporting a top-down, model-based design flow for real-time software in Cyber-Physical Systems.
- 2) We provide a methodology to statically schedule and compile a subset of LF into PRETVM bytecode.
- 3) We show that our approach is amenable to predicting the worst-case execution time (WCET) of systems’ hyperperiods.
- 4) We evaluate our approach using a set of LF benchmarks evaluating our methodology *w.r.t.* timing accuracy. Results show that PRETVM delivers time-accurate deterministic execution.

II. RUNNING EXAMPLE

A. Reaction Wheel System

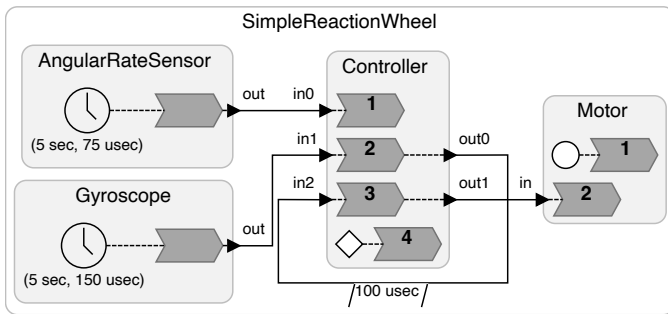


Fig. 1: A simple reaction wheel system

To informally introduce the reactor model, we present a simplified example of a reaction wheel system used for satellite attitude control [10]. In this system, a gyroscope and an angular rate sensor periodically collect data from the

environment and send them to a controller, which performs sensor fusion and generates a command the motor.

The diagram in Figure 1 represents the simplified reaction wheel system. A **reactor** is a stateful concurrent component. In the diagram, reactors are represented as rectangles with rounded corners, and they are Gyroscope, AngularRateSensor, Controller, and Motor. A reactor can contain **reactions**, **timers**, **ports**, and **connections**.

A reaction is a routine that executes when any of its triggers is present, and it is rendered as a chevron in the diagram. The body of a reaction is written in a **target language** and represents the “business logic” of the application. In this work, each reaction is further annotated with its worst-case execution time (WCET) for a given platform. The Controller reactor has four reactions, each labelled with an integer number. These numbers correspond to the **priorities** of the reactions within Controller, which determine the order in which reactions execute should they be triggered simultaneously. It is important to note that reaction priorities establish a total order only *within* the same reactor.

A reaction can be triggered by a port, a timer, an action, or a built-in trigger such as startup or shutdown. A port, rendered as a black triangle in the diagram, is used to communicate with other reactors. A timer, rendered as a clock in the diagram, is used to generate periodic events. Timers are characterized by an offset and a period which are shown below the clock. For example, the timer in AngularRateSensor starts firing at 5s with a period of 75s.

Around the Controller reactor, a connection is drawn from its output port out0 to its input port in2, with a delay of 100 μ s, effectively scheduling an event within itself 100 μ s into the future. The delay annotated to connections is optional. If no delay is specified, the event travels along a connection logically instantaneously.

The built-in trigger startup, rendered as a white circle, is present at the beginning of the execution, and the built-in trigger shutdown, rendered as a white diamond, is present at the last tag of the execution. Besides triggers, connections can be drawn between two ports using connection statements.

All events in the system are handled in the order of **tags**, which use a super-dense representation of time [11], encoded as tuples of the form $g = (t, m)$, where $t \in \mathbb{T}$ is the **time value** and $m \in \mathbb{N}$ is a **microstep index**. Reactions are logically instantaneous; **logical time** does not elapse during the execution of a reaction (**physical time**, denoted as T , on the other hand, does elapse). If a reaction produces an output that triggers another reaction, then the two reactions execute logically simultaneously (*i.e.*, at the same tag).

III. BACKGROUND

A. Reactor Model and Lingua Franca

The reactor model [6] is a deterministic model of concurrent computation for reactive systems. It is an adaptation of the actor model [12] in which messages flow through ports, and delivery is not address-based but connection-based, like in dataflow [13], [14] and Kahn process networks [15]. Messages

are tagged with a timestamp and delivered in order, assigning a discrete-event semantics to the operation of reactors. Unlike LET [16], in which logical execution time is synonymous with physical time, reactions to events are logically instantaneous, following the synchronous hypothesis that is central to the synchronous languages [17]. Still, a LET can be assigned to a reaction, simply by adding a logical delay to its output. The execution semantics of reactors ensure that at any tag, no reaction executes before all events that it depends on are known. This invariant is independent of the physical time that elapses during the execution of a reactor program, and it ensures that reactors behave deterministically. The proximity between the tag at which an event is scheduled and the physical time at which it is reacted to, *does* depend on execution times, and requires further analysis in order to provide any assurances in that regard.

LF is a polyglot coordination language that allows for the definition and composition of reactors. Event-triggered reactions, which constitute the functionality of reactors, have an interface specified in LF syntax, but an implementation specified in plain target code. Currently, LF supports C, C++, Python, Rust, and TypeScript. LF code gets compiled down to target code that is executable using a runtime environment that coordinates the scheduling of events and reactions to events. For most targets, the runtime transparently exploits available parallelism and utilizes multiple cores. LF has support for multiple platforms, including POSIX, Arduino, Zephyr, and several bare-iron microcontrollers. LF programs can also be federated, meaning that the reactor semantics get preserved in a distributed system, across separate processes that communicate over a network. Such federated execution is outside the scope of this paper.

B. Directed Acyclic Graphs (DAGs)

DAGs are widely used in real-time applications, such as automotive and avionics, to model real-time computing tasks and their precedence constraints. This subsection introduces basic concepts and notations for real-time DAG task modeling.

1) *Task Model*: A DAG task is characterized by (\mathcal{G}, P) , in which \mathcal{G} is a graph defining the set of sub-tasks and P denotes the DAG task period. The graph \mathcal{G} comprises of $(\mathcal{V}, \mathcal{E})$, where $\mathcal{V} = \{v_i\}$ is a set of n nodes representing n sub-tasks, and $\mathcal{E} = \{e_{ij}\}$ is a set of directed edges representing the precedence relation between the sub-tasks. For any two nodes v_i and v_j connected by a directed edge e_{ij} , v_j can start execution only if v_i has finished its execution. Given the edge e_{ij} , v_i is the predecessor of v_j . Each sub-task v_i is a non-preemptable sequential computing workload, with its worst-case execution time (WCET) denoted as C_i .

2) *Node-level Timing Attributes*: The timing constraints of each node can be defined through four attributes: earliest starting time (EST), earliest finishing time (EFT), latest starting time (LST), and latest finishing time (LFT). The EST is the earliest time a node can start executing, equalling the maximum of its predecessors' EFTs. Similarly, the LFT defines the latest time a node is allowed to finish its execution to meet

the deadline, which is equal to the minimum of its successors' LST. The relationship between the timing attributes is

$$\begin{aligned} t_i^{\text{EST}} &= \max\{t_j^{\text{EFT}} \mid e_{ji} \in \mathcal{E}\} \\ t_i^{\text{LFT}} &= \min\{t_j^{\text{LST}} \mid e_{ij} \in \mathcal{E}\} \end{aligned} \quad (1)$$

and $t_i^{\text{EFT}} = t_i^{\text{EST}} + C_i$ and $t_i^{\text{LST}} = t_i^{\text{LFT}} - C_i$. The t_i^{LFT} of all nodes without a successor is set to the DAG task period P .

C. DAG Modeling for LF Programs

When constructing the DAG task for DAG scheduling it is necessary that all externally defined constraints are represented through the DAG topology and the scalar node values. A real-time LF program releases a task v_i (i.e., a reaction invocation) at a time offset O_i and expects it to complete by a deadline D_i , where D_i could be the release time of the reaction's next invocation or the end of the hyperperiod. The DAG needs to be adapted to reflect these constraints, which are translated to constraints on node-level timing attributes as

$$O_i \leq t_i^{\text{EST}} \quad \text{and} \quad t_i^{\text{LFT}} \leq D_i, \quad (2)$$

i.e., the earliest starting time needs to be larger than the offset and the last finishing time needs to be less than the deadline. To constrain the timing attributes accordingly, we borrow the concept of **virtual nodes** from [18]. There are two types of virtual nodes, **dummy nodes** d_l that have a predefined execution time and **sync nodes** s_l with zero execution time. Using the virtual nodes, a **virtual path** can be constructed, alternating S sync and $S-1$ dummy nodes. The total execution time of the virtual path is equal to the period of the DAG task. Through the defined execution time of the dummy nodes, it follows that for each sync node s_l ,

$$t_{s_l}^{\text{EST}} = t_{s_l}^{\text{EFT}} = t_{s_l}^{\text{LST}} = t_{s_l}^{\text{LFT}} = \sum_{i=1}^{l-1} C_{d_i} = P - \sum_{j=l}^{S-1} C_{d_j}. \quad (3)$$

The nodes in the virtual path can be designed such that all unique offset and deadline values are represented by a sync node. Adding an edge from the appropriate sync node s_l to a sub-task v_k , or vice-versa, respectively, results in the relation

$$O_k = t_{s_l}^{\text{EFT}} \leq t_k^{\text{EST}} \quad \text{or} \quad t_k^{\text{LFT}} \leq t_{s_l}^{\text{LST}} = D_k, \quad (4)$$

which enforces (2) within the DAG task. As a concrete example, Figure 4 shows the DAG encoding of the running example.

IV. FROM LF TO QUASI-STATIC SCHEDULES

Let us now dive into our methodology, as shown in Figure 2. At a high level, our methodology consists of two parts: first, compiling an LF program into quasi-static schedules (Sec. IV), and second, generating and executing bytecode on PRETVM implementations (Sec. V). In this section, we focus on the first part, which covers the blue and brown boxes in Figure 2.

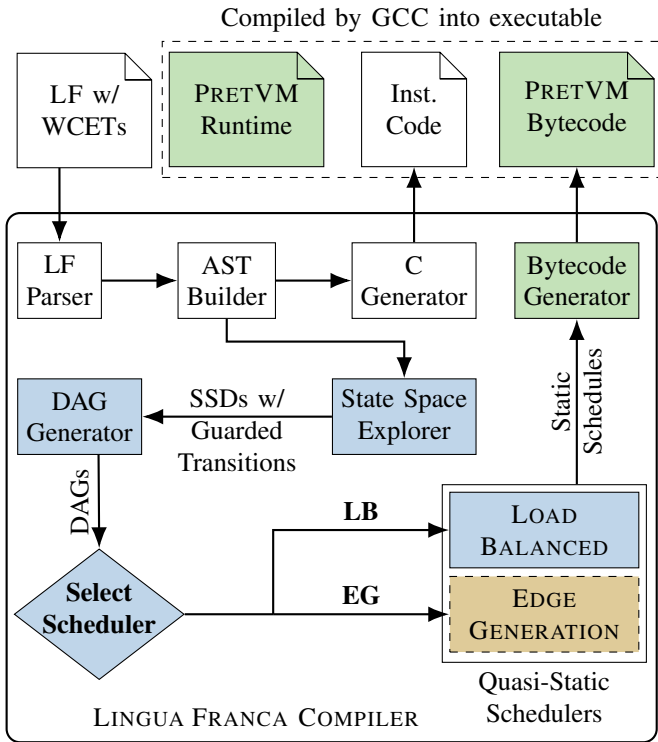


Fig. 2: Methodology overview. Colored boxes are our work. Brown boxes denote external tools we build interface for. Blue and brown boxes are described in Sec. IV. Green boxes are described in Sec. V.

A. State Space Diagrams with Guarded Transitions

The input of our approach is an LF program with WCET annotations. Each reaction is labeled by the user with a WCET annotation, indicating the maximum amount of time this reaction is expected to require to complete execution on a certain execution platform along with the associated overhead. We explain further in Sec. VI how a user could derive the WCETs. Given an annotated LF program, the LF compiler parses the program and builds an abstract syntax tree (AST). Once an AST is built, the compiler invokes a built-in C Generator for generating program-specific instrumentation code, including custom C structs for reactor definitions in the specific program, user-specified reaction bodies written in C, memory allocation and deallocation functions, etc.

From the AST, the **State Space Explorer** generates **State Space Diagrams** (SSDs) [19], which capture the logical behavior of an LF program. Lin et al. [19] identified a subset of LF programs whose logical behavior can be represented using a single SSD. In this work, we expand this subset of LF programs by combining multiple SSDs with guarded transition relations between each pair of SSDs.

An SSD is a directed graph (V, E) , where each node consists of a timestamp, a set of reactions invoked at this timestamp, and a set of future events known at this timestamp. Formally, $V = (t, r, e) \subseteq \text{tags} \times \mathcal{P}(\text{rxns}) \times \mathcal{P}(\text{events})$ and $E \subseteq V \times V$, where \mathcal{P} denotes a power set, tags denotes the

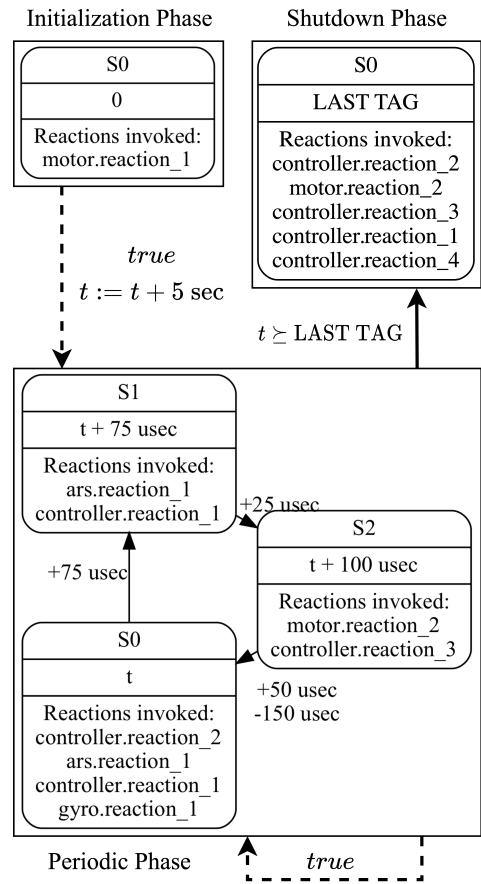


Fig. 3: Three separate SSDs connected by guarded transitions from the running example. Pending events are not rendered here to save space.

set of timestamps, rxns denotes the set of reactions in an LF program, and events denotes the set of events. To construct an SSD, the State Space Explorer performs a light-weight simulation by unrolling a worst-case execution until either

- 1) there are no more pending events, *i.e.*, $e = \emptyset$,
- 2) or the simulation completes a user-specified time horizon h , *i.e.*, $t = h$,
- 3) or a hyperperiod (*i.e.*, a cycle) is found.

The simulation approach is similar to [20].

In this work, we combine multiple SSDs to represent more dynamic behaviors of LF programs. Figure 3 shows the SSDs for the running example in Sec. II. The logical behavior of the reaction wheel system can be divided into three phases: an **initialization phase**, a **periodic phase**, and a **shutdown phase**. Each phase can be represented by an individual SSD, respectively. The initialization phase consists of one state space node with timestamp 0, the very first timestamp of an execution, and a single reaction invocation, reaction 1 from the Motor reactor, due to the startup trigger (rendered as a white circle in Figure 1). Similarly, the shutdown phase of the execution also consists of a single state space node with the last tag of the execution—a user-specified timeout—and

five possible reaction invocations due to the shutdown trigger and the last firings of the timers. The periodic phase contains three state space nodes: the first node starts at $t = 5s$, the second starts $75\mu s$ later, and the third node starts $25\mu s$ after the second. The reaction invocations occur due to the timer firings and the production of outputs from the reactions in the AngularRateSensor and Gyroscope.

The three phases of execution are connected using guarded transitions. Here, we use the arrow notations from [21], where the solid arrows represent regular guarded transitions, and dashed arrows represent *default* transitions, which are taken when none of the guarded transitions are taken. In Figure 3, the initialization phase has a default transition to the periodic phase, meaning that when the task set in the initialization phase is done, the execution can move onto the task set in the periodic phase. As part of the transition, the current time t is incremented by 5sec due to the five-second timer offset specified in the program (Figure 1). The periodic phase has two outgoing transitions. The first is a guarded transition to the shutdown phase, with a guard $t \geq \text{LAST TAG}$, where t denotes the current time. This transition is taken when the current time t reaches LAST TAG, which is a user-specified timeout value. While LAST TAG is not reached, the execution does not take this guarded transition, but instead takes the default transition of the periodic phase and executes the periodic task set for another hyperperiod.

B. Converting SSDs to DAGs

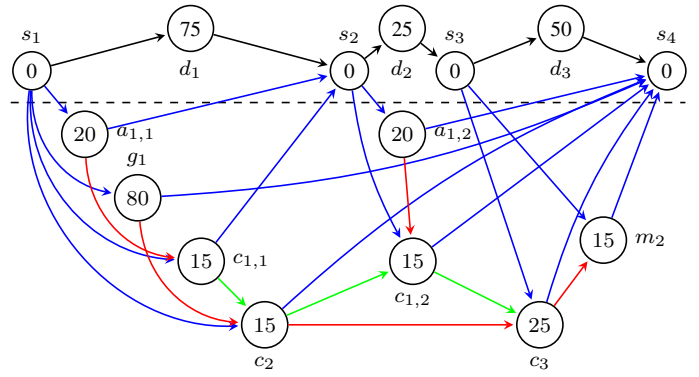
In Figure 2, after the SSDs with guarded transitions are generated by the State Space Explorer, the SSDs enter the DAG Generator and are converted to DAGs. The conversion starts by generating nodes corresponding to the reaction invocations, and then connects these nodes through edges based on timing and precedence constraints.

When iterating over the state space diagram, for each reaction invocation a node is generated, taking the current logical time as offset, and adopting the execution time of the reaction. In this work, we assume implicit deadlines for all nodes, meaning their deadline is equal to their period. As such, every node has a deadline according to the logical tag of its next invocation. The period of the DAG task is extracted from the length of the loop in the state space diagram. After generating all nodes, the virtual nodes are generated according to the unique offset and deadline values.

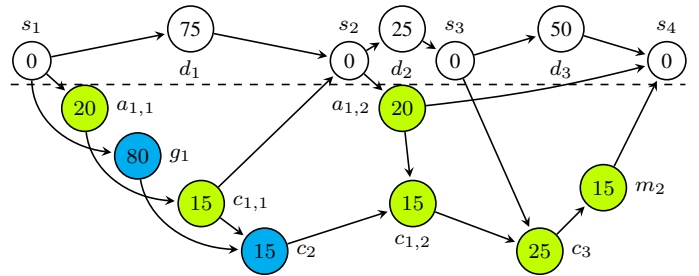
The edges added are the following:

- 1) Edges connecting the virtual nodes to form the virtual path;
- 2) Timing edges from and to the virtual path for offset and deadline values of the nodes, respectively;
- 3) Dependency edges between nodes corresponding to reactions where the second is triggered by the first;
- 4) Sequentialization edges between nodes belonging to the same reactor, ordering them by logical time, with the reaction number as tiebreaker.

Figure 4a shows the DAG generated from the periodic phase of Figure 3.



(a) DAG representation after conversion from the state space diagram in Figure 3, showing timing edges in blue, trigger edges in red, and reactor sequentialization edges in green, with the virtual path above the dashed line.



(b) Sample output from the EDGE GENERATION scheduler, which is a transitive reduction of the DAG in Figure 4a with width $M = 2 + 1$, with $+1$ for the virtual path. The colors of the nodes show a valid partitioning to 2 available cores.

Fig. 4: DAG generation and partitioned scheduling. The node names are the initial of the reactor name with the reaction number and optionally the invocation count as subscript. For example, $a_{1,1}$ is the first invocation of reaction 1 in AngularRateSensor. The numbers in the nodes indicated the WCET of each reaction and the nodes above the dashed line are the virtual path.

As an example for all the added edges, we focus on the node c_2 , which is the second reaction of the controller reactor. It received the attributes $O_{c_2} = 0$, $D_{c_2} = 150$, and $C_{c_2} = 15$ from the LF program. The blue edges from s_1 and to s_4 set the bounds for the timing attributes. The red edge from g_1 is added because the first reaction of the gyroscope triggers this reaction. The green edge from $c_{1,1}$ is added because the first instance of the first reaction of the controller reactor has the same logical tag but lower number. The outgoing green edge to $c_{1,2}$ is set because it has a higher logical tag. Lastly, the red outgoing edge to c_3 is added because c_3 is triggered by c_2 through the logical action. An example for the need of the virtual path can be seen when inspecting the node c_3 . Due to the logical action with a minimum delay of 100 the offset of the reaction should be $O_{c_3} = 100$, necessitating the constraint $t_{c_3}^{EST} \geq 100$. By adding the edge from the sync node s_3 , c_3 cannot start before 100 due to the total time required by d_1 and d_2 .

C. Scheduling by Graph Partitioning

After the conversion to DAGs, the LF compiler selects a user-specified quasi-static scheduler and feed the generated DAGs to it. At a high level, a quasi-static scheduler takes a set of graphs as input, partitions the graphs based on the number of workers available, and outputs graph partitions, which are considered as **quasi-static schedules**—a spatial mapping between tasks and execution platforms with timing and inter-task dependencies. The schedules are quasi-static because they statically encode tasks that *could* be triggered, but whether they are actually triggered is determined during execution using virtual instructions facilitating control flow. More details on these instructions are explained in Sec. V.

Given an unpartitioned DAG, a quasi-static scheduler is free to designate DAG nodes to any partition it deems fit. The scheduler can modify edges as long as the output partitioned DAG satisfies all dependencies in the input unpartitioned DAG. In addition, the quasi-static scheduler must linearize each partition by adding edges such that there exists a path in the output DAG passing through all nodes within the same partition.

In this work, we support two different types of schedulers: LOAD BALANCED and EDGE GENERATION [9]. The LOAD BALANCED scheduler is a complete scheduler implemented in Java, embedded inside the LF compiler. It directly takes the generated DAGs as input and produces graph partitions that aim to assign each worker the same amount of work measured in execution times.

The EDGE GENERATION scheduler, on the other hand, is an external static scheduler implemented in Python by Sun et al. [9]. Instead of distributing workloads fairly across workers, EGS focuses on satisfying timing constraints. Given a DAG task with a deadline, EGS checks whether the DAG task is *trivially schedulable* on the given number of processors. A DAG task (\mathcal{G}, P) is trivially schedulable on M processors if its length is less than or equal to the period P and its width is less than or equal to the number of processors M . If it is not trivially schedulable by construction, EGS adds edges trying to make it trivially schedulable. A trivially schedulable DAG can easily be partitioned using paths that cover the DAG, with an example shown in Figure 4b.

V. FROM QUASI-STATIC SCHEDULES TO PRETVM

Once quasi-static schedules are generated in the form of graph partitions, they will then be compiled into bytecode and executed by the PRETVM runtime. This section walks through the green boxes in Figure 2 in detail. The main challenges we address here include composing virtual instructions to deliver correct LF semantics (*i.e.*, deterministic concurrency) and accounting for LF’s generality over LET (*i.e.*, encoding the logical timeline and detecting whether a reaction should be invoked during execution), while maintaining low overhead.

A. Virtual Instruction Set

We begin by defining a virtual instruction set for PRETVM, which is used to encode the quasi-static schedules. The full

TABLE I: PRETVM Virtual Instruction Set

Instruction	Description
ADD op1, op2, op3	Add to an integer variable (op2) by an integer variable (op3) and store to a destination register (op1).
ADDI op1, op2, op3	Add to an integer variable (op2) by an immediate (op3) and store to a destination register (op1).
ADV op1, op2, op3	Advance the logical time of a reactor (op1) to a base time register (op2) + a time increment variable (op3).
ADVI op1, op2, op3	Advance the logical time of a reactor (op1) to a base time register (op2) + an immediate value (op3).
BEQ op1, op2, op3	Take the branch (op3) if the op1 register value is equal to the op2 register value.
BGE op1, op2, op3	Take the branch (op3) if the op1 register value is greater than or equal to the op2 register value.
BLT op1, op2, op3	Take the branch (op3) if the op1 register value is less than the op2 register value.
BNE op1, op2, op3	Take the branch (op3) if the op1 register value is not equal to the op2 register value.
DU op1, op2	Delay until the physical clock reaches a base timepoint (op1) plus an offset (op2).
EXE op1, op2	Execute a function (op1) with argument (op2).
JAL op1 op2	Store the return address to op1 and jump to a label (op2).
JALR op1, op2, op3	Store the return address to op1 and jump to a base address (op2) + an immediate offset (op3).
STP	Stop the execution.
WLT op1, op2	Wait until a register value (op1) to be less than a desired value (op2).
WU op1, op2	Wait until a register value (op1) to be greater than or equal to a desired value (op2).

instruction set is shown in Table I.

The PRETVM is a register-based virtual machine. The virtual instruction set borrows inspiration from the RISC-V instruction set [22] and the timing instructions from the PRET Machines [23]–[25]. The virtual instruction set contains standard RISC-V-like instructions such as ADD, ADDI, BEQ, BGE, BLT, BNE, JAL, and JALR. These instructions are useful for encoding control flow and manipulating auxiliary registers (further explained in Sec. V-B) that keeps track of the progress of a quasi-static schedule.

Besides the standard instructions, the virtual instruction set also contains timing instructions, including DU, WU, and WLT. The use of timing instructions adopts the PRET philosophy of making timing a *semantic* property of the instruction set. The DU instruction helps align an execution with real time, and the WU and WLT instructions are useful for implementing synchronization among workers.

Lastly, we introduce reactor-inspired instructions: ADV, ADVI, EXE, and STP. The ADV and ADVI instructions advance the timestamp of a reactor’s state. EXE executes a C function pointer, which could be a user-written reaction body or any functions required by the runtime to deliver the LF semantics. STP terminates the LF program execution.

B. Generating Bytecode from Quasi-Static Schedules

With a virtual instruction set defined, we are almost ready to encode the quasi-static schedules, *i.e.*, partitioned graphs, into bytecode, which consists of sequences of virtual instructions,

one for each worker thread. Before we dive into the main instruction generation algorithm, let us walk through a few prerequisites for encoding the quasi-static schedules using the virtual instruction set.

a) Auxiliary Registers: Encoding the semantics of quasi-static schedules requires storing certain information at runtime in registers. Certain types of registers are worker-specific, meaning that they are duplicated for each worker, while others are global, meaning that they are unique and read by all workers. The progress of a worker during the execution of its schedule is tracked using a worker-specific `counter` register. A global `start_time` register keeps track of the timestamp at which the execution starts, while a global `timeout` register stores the last timestamp (*i.e.*, the timestamp in the shutdown phase in Figure 3) of the execution, as specified by the user. We use a global `time_offset` register to keep track of the timestamp at the beginning of the current hyperperiod. To increment `time_offset` by a variable amount, as the execution goes through different phases, a global `offset_inc` register is used to store these variable increments at different points during the execution. To store the return address of a worker before a jump, we use a worker-specific `return_addr` register. Moreover, for the purpose of global synchronization at the boundary of a hyperperiod (explained later), each worker uses a `binary_sema` register as a binary semaphore. Lastly, there is a global constant `zero` register, which always holds a value of 0.

b) Synchronization: In our execution strategy, we support two types of synchronization: (i) **local synchronization** between a pair of workers, and (ii) **global synchronization** across all workers. Local synchronization is achieved using the `WU` and the `counter` registers. Without loss of generality, assume that worker *B* needs to wait until worker *A* completes some upstream task. To implement this, in worker *A*'s bytecode, we use an `ADDI` to increment worker *A*'s `counter` after it completes the upstream task, and in worker *B*'s bytecode, we use a `WU` to let it block until worker *A*'s `counter` reaches the incremented value. On the other hand, global synchronization across all workers is achieved by inserting a **synchronization code block** into each worker's bytecode. One worker is designated as the **coordinator**, denoted as *c*, facilitating the global synchronization, while the other workers are **participants**. Each participant is denoted as *p*. The coordinator executes the following code block:

```

1) WU binary_semap, 1
2) (... Repeat WU for each participant p ...)
3) ADD time_offset, time_offset, offset_inc
4) ADDI counterc, zero, 0
5) ADDI counterp, zero, 0
6) (... Repeat ADDI for each participant p ...)
7) ADVI reactor, time_offset, 0
8) (... Repeat ADVI for each reactor in the LF program ...)
9) ADDI binary_semap, zero, 0
10) (... Repeat ADDI for each participant p ...)
11) JALR zero, return_addrc, 0

```

Conversely, each participant executes this shorter code block:

```

1) ADDI binary_semap, zero, 1
2) WLT binary_semap, 1
3) JALR zero, return_addrp, 0

```

During global synchronization, the coordinator first waits until all participants have entered their own sync. blocks (line 1-2). A participant enters the sync block and notifies the coordinator by setting its `binary_sema` to 1 (line 1 in the participant code below). Once they have entered and get blocked by the `WLT` (line 2 below), the coordinator then updates the global hyperperiod offset (line 3 above), resets all workers' `counter` registers (line 4-6), and advances the timestamp of all reactors' states (line 7-8). Once these "bookkeeping" procedures are done, the coordinator resets the `binary_sema` registers to 0 (line 9-10 above), at which point the participants are unblocked by `WLT` and jump back to the return addresses specified in their `return_addr` registers (line 3 below).

c) Connections: LF allows the user to specify connections with optional fixed logical delays. When the delays are greater than the rate at which output ports are written, a storage layer is required to store the in-flight events. In this work, we implement a connection buffer for each delayed connection using a fixed-size circular buffer. Since the LF semantics guarantees that events sent along a connection have monotonically increasing timestamps, there is no need to reorder events and hence circular buffers suffice.

For each connection, we code-generate two **connection helper functions**: a pre-connection helper function pushes an event into the circular buffer, and a post-connection helper function pops an event from the circular buffer. The quasi-static schedule executes connection helper functions using the `EXE` instruction. Since the LF semantics allows an output port to be written to by multiple reactions triggered at the same timestamp, with the last reaction taking precedence, a pre-connection helper is inserted after invoking the last reaction that could modify this port to push the latest written value into the connection buffer. If a reaction is triggered by a port, a post-connection helper is inserted to pop the stale value read by the reaction from the connection buffer.

If a connection has no delay, we optimize the connection helper functions away and let the downstream receiving reaction read value directly from the pointer to the sending reactor's output port.

d) Trigger Detection: The LF semantics requires a reaction to be invoked when *any* of its triggers becomes present. Since it is unknown at compile time whether an input-triggered reaction does get triggered during execution, the quasi-static schedule must encode logic for checking the presence of triggers at runtime. We implement the trigger detection mechanism using a combination of `BEQ`, `JAL`, and `EXE`. For every trigger a reaction has that is an input port, a `BEQ` is generated. If the input port is connected to a delayed connection, the `BEQ` checks if the head event of the connection buffer has the same timestamp as the current timestamp of the reaction's parent reactor. Otherwise if the input port is connected to a zero-delay connection, the `BEQ` checks if the sending output port's `is_present` field is `true`. In both cases, when the condition

evaluates to true, the `BEQ` branches to the location of an `EXE` instruction invoking the reaction body. After a list of `BEQ` is generated, a `JAL` instruction is generated, which branches to the instruction *after* the reaction-invoking `EXE`, when all triggers are absent, in which case the reaction-invoking `EXE` is bypassed. A concrete example of this mechanism is shown in Figure 5 (line 4-6).

e) Instruction Generation: Having discussed the above prerequisites for generating bytecode that encodes quasi-static schedules, we are now ready to dive into Algorithm 1, which shows the procedure for generating virtual instructions from a partitioned graph.

Algorithm 1 Generate Instructions from a Partitioned Graph

```

1: procedure GENERATEINSTRUCTIONS(graphPartitioned)
2:   Let  $B_i$  be the set of instructions for worker  $i$ 
3:   Let  $W$  be the total number of workers
4:   Topologically sort the DAG nodes by dependencies
5:   for all  $\text{currentNode} \in \text{topologicalSort}$  do
6:      $w \leftarrow \text{currentNode.assignedWorker}$ 
7:     if  $\text{currentNode.type} = \text{reaction}$  then
8:       for all upstream reactions of  $\text{currentNode}$  do
9:          $B_w \leftarrow B_w \cup \{\text{WU}\}$   $\triangleright$  Wait for upstream
10:      end for
11:      if  $\text{currentNode}$  depends on sync node then
12:        GENERATEPRECONNECTIONHELPERS()
13:         $B_w \leftarrow B_w \cup \{\text{ADV1}, \text{DU}\}$ 
14:      end if
15:      for all input port triggers of  $\text{currentNode}$  do
16:         $B_w \leftarrow B_w \cup \{\text{BEQ}\}$   $\triangleright$  Test trigger presence
17:      end for
18:       $B_w \leftarrow B_w \cup \{\text{JAL}\}$   $\triangleright$  Absent triggers, skip EXE
19:       $B_w \leftarrow B_w \cup \{\text{EXE}\}$   $\triangleright$  Execute reaction
20:      GENERATEPOSTCONNECTIONHELPERS()
21:       $B_w \leftarrow B_w \cup \{\text{ADDI}\}$   $\triangleright$  Update counter
22:    else if  $\text{currentNode.type} = \text{sync}$  and  $\text{currentNode}$  is tail
node of DAG then
23:      GENERATEPRECONNECTIONHELPERS()
24:      if  $\text{currentNode.time}$  is not  $\infty$  then
25:        for  $i = 0$  to number of workers - 1 do
26:           $B_i \leftarrow B_i \cup \{\text{DU}\}$   $\triangleright$  End of hyperperiod
27:          if  $i = 0$  then
28:             $B_i \leftarrow B_i \cup \{\text{ADDI}\}$   $\triangleright$  Iterate again
29:          end if
30:           $B_i \leftarrow B_i \cup \{\text{JAL}\}$   $\triangleright$  Synchronize
31:        end for
32:      end if
33:    end if
34:  end for
35:  return  $\bigcup_{i=0}^{W-1} B_i$ 
36: end procedure

```

The algorithm first topologically sorts the nodes of the partitioned graph and traverses the graph in the sorted order, ensuring that before visiting a node, all of its dependencies have been already visited. If the current node is a reaction node, then a `WU` is generated for each of its upstream tasks. Moreover, if the reaction node depends on a *sync* node, pre-connection helper functions are first generated for earlier reactions that write to output ports; then, `ADV1` and `DU` instructions are generated to advance the timestamps of the parent reactor and delay the execution until the physical release time of

the reaction node. Then, instructions for trigger detection are generated, which start with a sequence of `BEQ` instructions and a `JAL` instruction. This is then followed by an `EXE` instruction for executing the reaction body. Once the reaction is executed, a sequence of `EXE` instructions execute the post-connection helper functions. An `ADDI` instruction is then used to increment a worker counter, effectively updating the current progress of the worker. If the current node is an *sync* node and is the tail node of the partitioned graph, then pre-connection helper functions are generated for all the remaining reactions invoked in the current hyperperiod, which can write to output ports. A `DU` is also added to each worker’s bytecode. Each worker further uses an `ADDI` to increment the hyperperiod register. Once that is done, each worker executes a `JAL` to the synchronization block.

f) Linking: Once a sequence of instructions is generated for each partitioned graph for each worker, the Bytecode Generator links multiple sequences together into a single piece of output bytecode. The linking process proceeds by phases. It starts with the first phase the execution enters into, such as the initialization phase, and places the generated instructions from this phase into the output bytecode. Then, the process follows the guarded transitions and places the generated instructions from downstream phases one-by-one, until there are no more unlinked phases with incoming transitions. At the end of the instructions generated by each phase, the Bytecode Generator places instructions generated from guarded transitions using `JAL` and branch instructions. In the running example (Figure 3), the default transition between the initialization phase and the periodic phase is encoded as a `JAL` instructions between two code blocks corresponding to the two phases, similarly for the default self transition in the periodic phase. The guarded transition with the guard $t \succeq \text{LAST TAG}$ is encoded as `BGE t, LAST TAG, SHUTDOWN`.

Finally, as a concrete example, the generated bytecode for the worker assigned to the blue partition in Figure 4b is shown in Figure 5.

- 1) `EXE g1` (This line is labeled `PERIODICblue`.)
- 2) `ADDI counterblue, counterblue, 1`
- 3) `WU countergreen, 2`
- 4) `BEQ inl_is_present, true, line_6`
- 5) `JAL line_9`
- 6) `EXE c2`
- 7) `EXE out0_pre_connection_helper`
- 8) `EXE inl_post_connection_helper`
- 9) `ADDI counterblue, counterblue, 1`
- 10) `DU time_offset, 150μs`
- 11) `ADDI offset_inc, 150μs`
- 12) `JAL return_addrblue, SYNC_BLOCK`
- 13) `BGE time_offset, timeout, SHUTDOWNblue`
- 14) `JAL return_addrblue, PERIODICblue`

Fig. 5: Generated bytecode for the blue worker in Figure 4b

C. Executing Bytecode on PRETVM

At this point in the workflow (Figure 2), we have finished generating the PRETVM bytecode. To execute the bytecode, we implement a PRETVM Runtime, which implements the virtual instruction set and interprets the bytecode during execution. To make the PRETVM Runtime compatible with the LF instrumentation code, we embed the runtime under the scheduler API of the LF runtime library. The PRETVM runtime, the instrumentation code, and the PRETVM bytecode is further compiled by a C compiler, such as GCC, into an executable.

VI. PREDICTABLE TIMING

Predictability is a central concern in real-time system design. In the literature, however, predictability is often subject to different interpretations. We argue that whether a system is predictable depends on the *prediction* one aims to make. Prior works have focused on finding the worst-case execution times (WCETs) of individual tasks on various platforms. However, finding a WCET at the system level, where tasks coordinate and execute concurrently on multicore platforms, remains an open problem.

An LF runtime based on PRETVM cleanly separates application logic (*i.e.*, reaction bodies) from coordination logic (*i.e.*, quasi-static schedules), presenting a practical way of writing real-time software that is amenable to timing analysis. On the one hand, LF reactions are run-to-completion at the time of writing, removing the need to account for preemption and thus simplifying timing analysis. On the other hand, PRETVM instructions' straightforward semantics simplifies the WCET analysis of each instruction.

Here we make a key assumption that the user can derive WCET values for each reaction body and every PRETVM instruction on a given platform, *e.g.*, using timing analysis tools or direct measurements. We treat these WCET values as *estimates*—they do not need to be ground truth, but violations of them are considered fault conditions handled at runtime. Assuming that the individual WCET estimates are not violated during execution, we can now predict the WCET of an LF program's hyperperiod, represented as a DAG and implemented in PRETVM bytecode.

We denote a time domain as \mathbb{T} . In practice, this domain is defined as $\mathbb{T} = \mathbb{Z}$, where the unit is nanosecond. Based on the previous assumption, the user can obtain WCETs for individual reaction bodies and PRETVM instructions, *i.e.*, there exists a function $w_r : \mathcal{R} \rightarrow \mathbb{T}$ and a function $w_i : \mathcal{I} \rightarrow \mathbb{T}$, where \mathcal{R} denotes the set of reactions and the \mathcal{I} denotes the set of PRETVM instructions. For the WCETs of `DU`, `WU`, and `WLT`, their wait time does not count toward the WCETs, only the overhead of calling these instructions does. Similarly for `EXE`, the WCET of the function its first operand points to does not count toward the WCET of the `EXE` instruction itself.

Definition VI.1 (WCET of a node). The WCET of a node n is a function $w : \mathcal{V} \rightarrow \mathbb{T}$ defined as

$$w(n) = \begin{cases} 0 & \text{if } n \text{ is } \textit{sync}, \\ d & \text{if } n \text{ is } \textit{dummy} \text{ with interval } d, \\ \sum_{i \in I(n)} w_i(i) + w_r(r) & \text{if } n \text{ is for reaction } r. \end{cases}$$

where $I : \mathcal{V} \rightarrow \mathcal{P}(\mathcal{I})$ returns the set of PRETVM instructions generated by a given node n .

Referring back to the running example, node g_1 in Figure 4b generates line 1-2 in Figure 5, so when the user provides a WCET annotation for the reaction in Gyroscope, the annotated WCET estimate should account for `EXE`, `ADDI`, and the reaction body in Gyroscope.

Lemma VI.1 (WCET up to node n). The WCET up to a node n , denoted recursively as $\bar{w}(n)$, is defined as

$$\bar{w}(n) = \begin{cases} w(n) & \text{if } U(n) = \emptyset, \\ \max_{u \in U(n)} \bar{w}(u) + w(n) & \text{otherwise.} \end{cases}$$

where $U : \mathcal{V} \rightarrow \mathcal{P}(\mathcal{V})$ maps a DAG node n to a set of its immediately upstream DAG nodes, and if n is the tail node, $U(n)$ excludes virtual nodes from the returned set.

Proof. We prove this theorem by induction. In the base case, the DAG has a single *sync* node n , which is also the tail node, and so its WCET, which is by construction 0, equals $w(n) = \bar{w}(n)$ since the tail node has no upstream. The base case therefore holds. In the inductive step, the DAG has more than one nodes and the tail node necessarily has upstream nodes, *i.e.*, $U(n) \neq \emptyset$. By the induction hypothesis, for each upstream node $u \in U(n)$, $\bar{w}(u)$ is the WCET up to node u . Since all upstream nodes point to the tail, a maximum of $\bar{w}(u)$ needs to be taken over all $u \in U(n)$. Given that the tail node n has a WCET of 0, the WCET up to the tail node equals $\max_{u \in U(n)} \bar{w}(u) + 0 = \max_{u \in U(n)} \bar{w}(u) + w(n) = \bar{w}(n)$. Therefore, the induction step holds. \square

Theorem VI.2 (WCET of a DAG task set). The WCET of a DAG with the tail node n_t is $\bar{w}(n_t)$.

Proof. The proof follows from Lemma VI.1. \square

Example 1. The WCET of the DAG in Figure 4b can be captured by $\bar{w}(s_4)$, where

$$\begin{aligned} \bar{w}(s_4) &= \max(\bar{w}(a_{1,2}), \bar{w}(m_2)) + w(s_4) \\ &= \max(\bar{w}(s_2) + 20, \bar{w}(c_3) + 15) + 0 \\ &= \max(\max(75, \bar{w}(c_{1,1})) + 20, \\ &\quad \max(\bar{w}(s_3), \bar{w}(c_{1,2})) + 40) \\ &= \dots = 150 \end{aligned}$$

VII. EVALUATION

We evaluate the *timing accuracy* of PRETVM by running a set of real-time LF benchmarks on Raspberry Pi 4 Model B running Linux. In this experiment, accuracy is measured

Program	LoC (LF)	Average (us)			Maximum (us)			Standard Deviation (us)		
		DY	LB	EG	DY	LB	EG	DY	LB	EG
Philosophers	314	18.4	12.1	11.9	355	99.2	510	9.99	5.65	9.33
LongShort	31	1.49e+06	3.11	3.17	2.91e+06	5.22	4.32	8.11e+05	0.781	0.571
CoopSchedule	54	18.5	10.9	12.3	50.4	32.2	69	7.64	4.69	6.4
Counting	179	14.6	6.81	6.74	76.8	42.4	51.5	5.95	2.74	2.99
ThreadRing	217	19.5	14.8	12.3	44.2	58.3	36.2	7.18	8.05	6.28
ADASModel	91	12.9	5.49	1.81e+03	41.6	19.4	1.2e+04	5.5	3.35	3.58e+03
PingPong	124	13.6	8.02	7.96	64.4	59.9	56.8	4.14	3.95	3.87
Throughput	166	16.2	13.6	14.1	29.1	33.4	30.5	5.18	6.87	7.04

TABLE II: Average, maximum, and standard deviation of the lags in microseconds of the dynamic scheduler (DY), the static LOAD BALANCED scheduler (LB), and the static EDGE GENERATION scheduler (EG).

in terms of the *lag* of reaction invocations. For a reaction invocation i , its lag, l_i , is defined as

$$l_i = T_i - t_i,$$

where T_i is the physical time at which the reaction invocation occurs and t_i the logical timestamp. Intuitively, the smaller the difference between the physical invocation time and the ideal logical invocation time, the more time-accurate an execution is. We run the same set of benchmarks using two static schedulers, LOAD BALANCED and EDGE GENERATION, and we compare their performance against LF’s default DYNAMIC SCHEDULER.

The eight benchmarks are selected from [19], [26] with a focus on concurrent actor design patterns [27], which can be found in modern Cyber-Physical Systems. For each benchmark program, we annotate each reaction’s WCET estimate using an `@wctet` attribute. Syntax elements which are currently not supported by our implementation include nested reactors, logical and physical actions, and multiports. A logical action is replaced by adding a connection that links two newly created output and input ports. The reactor hierarchy is flattened manually and multiports were expanded by hand.

We collect performance data using LF’s tracing utility, which embeds trace points throughout the codebase to inspect notable events in the runtime system. Each event contains an event type, a logical timestamp, and a physical timestamp. In this experiment, we only collect events for the starting points of reactions. This choice ensures that the overhead of tracing stays uniform for all three schedulers under test. To avoid distortions in our measurements, we have also increased the size of the trace buffer to minimize data being written to disk during execution.

LF schedulers need to wait for the physical time to surpass the next reaction invocation’s logical timestamp before processing the invocation. To ensure a fair comparison between the schedulers, we implement the wait mechanism in all three schedulers under test using busy wait, replacing the sleep mechanism found in the default dynamic scheduler. By doing this, we remove timing variation from operating system’s sleep mechanism and attribute the difference in performance to scheduler designs.

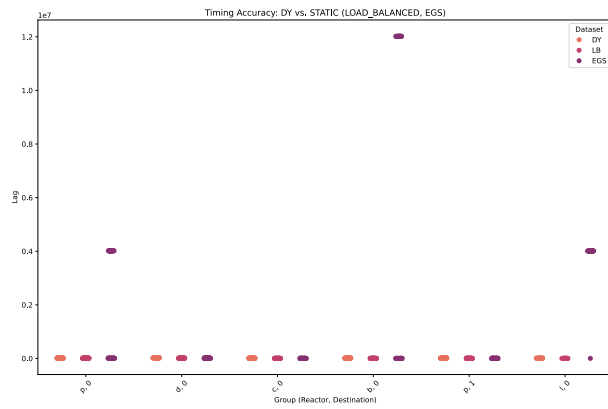
Table II shows an overview of the timing accuracy results. Compared to the dynamic scheduler, the static LOAD BAL-

ANCED scheduler has smaller average and maximum lags on all benchmarks, and it has a smaller standard deviation on all benchmarks except ThreadRing.

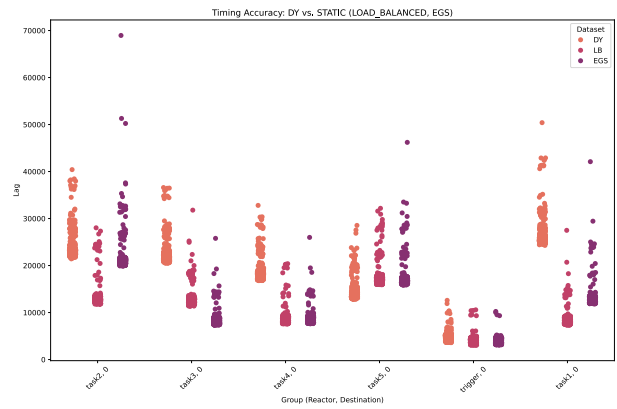
Figure 6 shows strip plots of lags during the periodic phase of each program. For most reactions, LOAD BALANCED and EDGE GENERATION have smaller lags than the dynamic scheduler. The occasional outliers shown in the strip plots can be due to several reasons, including interrupts from the underlying OS and the flushing of trace buffers to disk.

In ADASModel, EDGE GENERATION shows three clusters of outliers. This is due to EDGE GENERATION’s scheduling strategy involving adding edges to the DAG, which tends to delay the releasing of tasks in exchange for schedulability guarantees. We note that the goal of using EDGE GENERATION is not to minimize lags, but to use its analysis capability to ensure that a DAG is schedulable. In this case, larger lags from EDGE GENERATION seem tolerable. In general, LOAD BALANCED is better at minimizing lags than EDGE GENERATION and the dynamic scheduler.

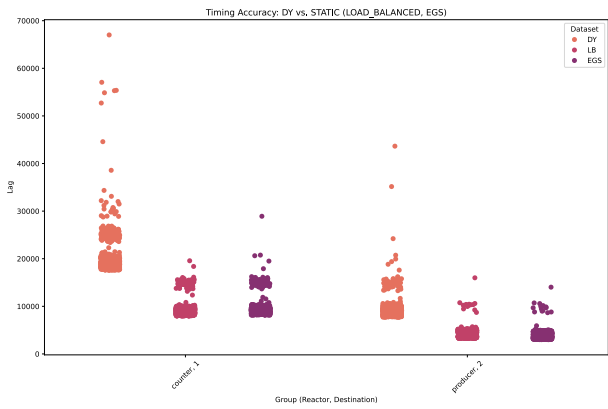
Notably, for the LongShort benchmark, LOAD BALANCED and EDGE GENERATION significantly outperform the dynamic scheduler. This performance gain can be explained by the fact that the quasi-static schedulers keep track of the current logical time for *each* reactor, meaning that every reactor can advance its logical time independently as long as the core LF semantics is respected, *i.e.*, each reactor processes events in timestamp order. The dynamic scheduler, on the other hand, uses a single variable to track logical time for *all* reactors, ensuring that all reactors advance time together. The LongShort benchmark has a design pattern that combines infrequent, long-running reactions with frequent, short-running reactions. The dynamic scheduler struggles because it performs a **global barrier synchronization** at the end of each tag. The barrier makes reactions that are to occur at the next tag wait on the long-running reactions, even if there are no more actual data dependencies to fulfill. In the quasi-static schedulers, the capability to advance time individually for each reactor effectively prevent waiting unnecessarily, resulting in significantly reduced lags. We plan to compare our PRETVM approach with ongoing research on easing global barrier synchronization in dynamic schedulers in the future.



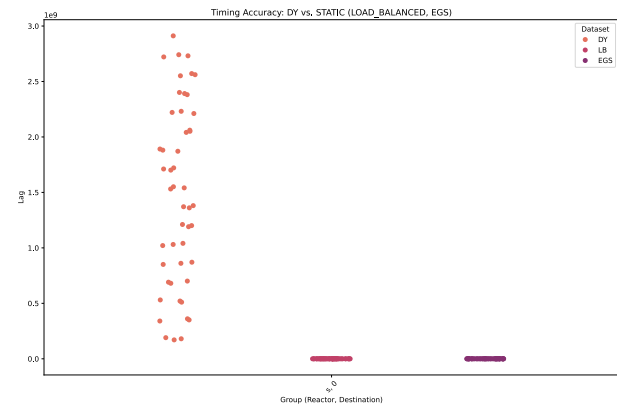
(a) ADASModel



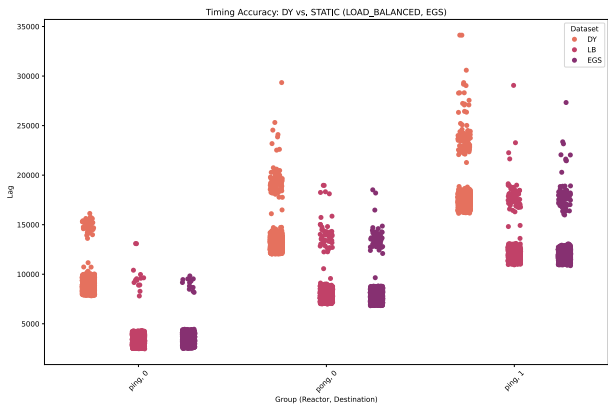
(b) CoopSchedule



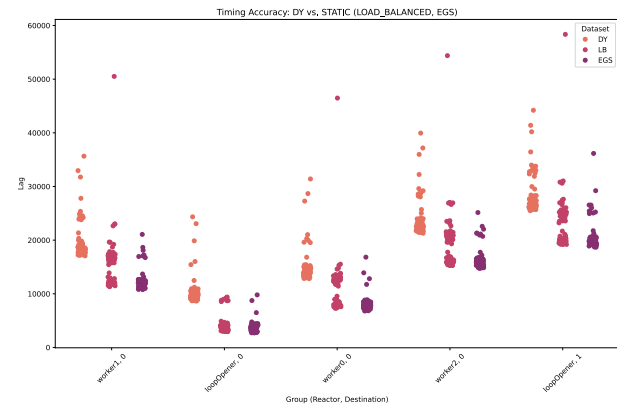
(c) Counting



(d) LongShort



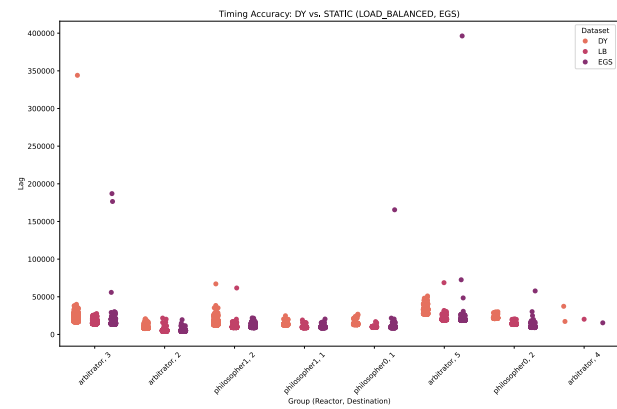
(e) PingPong



(f) ThreadRing



(g) Throughput



(h) Philosophers

Fig. 6: Timing accuracy benchmark results. X-axis shows reaction names. Each reaction contains three distributions, DY, LB, and EG, respectively. Y-axis is lag in nanoseconds.

VIII. RELATED WORK

Our work is largely inspired by the Embedded Machine [3], which serves as an execution backend for the Giotto language [2], [16], implementing the LET model [28]. An emerging extension of LET is the System-level LET (SL LET) model, which scales LET to distributed settings by introducing a notion of “time zones” [29]. The reactors model [6] in LINGUA FRANCA generalizes LET by distinguishing logical time from physical time [7]. Another emerging model offering similar generalization is the Sparse Synchronous Model (SSM) [30], the semantics of which can be facilitated using RP2040’s PIO instruction set [31], sharing similarity with our approach. The difference here is that it seems challenging to generate quasi-static schedules for SSM, while we show that it is feasible for a subset of LF.

In the real-time scheduling literature, various hardware and software complexities have been considered in real-time systems, leading to a range of Directed Acyclic Graph (DAG) representations. One of the earliest contributions to DAG scheduling introduced what is now known as Graham’s bound. It provides an upper bound on the response time of a task based on the longest path within the DAG and the DAG’s volume [32]. In recent years, He et al. [33] proposed a method of prioritizing subtasks within the longest paths to reduce response times and enhance schedulability. Subsequently, Zhao et al. [34] improved the priority assignment strategy at the subtask level by considering subtask dependencies. Different from the above approaches, Sun et al. [9] proposed a new DAG scheduler named Edge Generation Scheduling (EGS).

IX. CONCLUSION

In this paper, we present the Precision-Timed Virtual Machine, PRETVM, which facilitates the execution of quasi-static schedules compiled from a subset of LF programs, supporting a top-down, model-based design flow for real-time software in Cyber-Physical Systems. Our approach is amenable to predicting the WCETs of LF programs’ hyperperiods given assumptions on the WCETs of individual reactions and virtual instructions. We evaluate our approach using design patterns found in modern CPSs, implemented in LF. The results show that PRETVM delivers time-accurate deterministic execution.

ACKNOWLEDGMENT

The work in this paper was supported in part by the National Science Foundation (NSF), award #CNS-2233769 (Consistency vs. Availability in Cyber-Physical Systems), by DARPA grant FA8750-20-C-0156, by Intel, and by the iCyPhy Research Center (Industrial Cyber-Physical Systems), supported by Denso, Siemens, and Toyota.

This work was also supported, in part, by the German Federal Ministry of Education and Research (BMBF) as part of the program “Souverän. Digital. Vernetzt.”, joint project 6G-life (16KISK001K), and by the German Research Council (DFG) through the InterMCore project (505744711).

Mirco Theile and Binqi Sun were supported by the Chair for Cyber-Physical Systems in Production Engineering at TUM.

The authors thank Linh Thi Xuan Phan and the anonymous reviewers for providing helpful feedback. Shaokai Lin thanks Zitao Fang and Yang Huang for their collaboration on a course project for CS267 (Application of Parallel Computers) at UC Berkeley, which provided early inspiration for this work.

REFERENCES

- [1] Z. Liu, W. Zhang, and F. Zhao, “Impact, challenges and prospect of software-defined vehicles,” *Automotive Innovation*, vol. 5, no. 2, pp. 180–194, 2022.
- [2] T. A. Henzinger, B. Horowitz, and C. M. Kirsch, “Giotto: A time-triggered language for embedded programming,” *Proceedings of IEEE*, vol. 91, no. 1, pp. 84–99, 2003.
- [3] T. A. Henzinger and C. M. Kirsch, “The embedded machine: Predictable, portable realtime code,” in *International Conference on Programming Language Design and Implementation (PLDI)*. ACM Press, 2002, Conference Proceedings, pp. 315–326.
- [4] M. Lohstroh, C. Menard, S. Bateni, and E. A. Lee, “Toward a Lingua Franca for deterministic concurrent systems,” *ACM Transactions on Embedded Computing Systems (TECS), Special Issue on FDL’19*, vol. 20, no. 4, p. Article 36, May 2021.
- [5] M. Lohstroh, S. Bateni, C. Menard, A. Schulz-Rosengarten, J. Castrillon, and E. A. Lee, “Deterministic coordination across multiple timelines,” *ACM Transactions on Embedded Computing Systems (TECS)*, Oct. 2023. [Online]. Available: <https://doi.org/10.1145/3615357>
- [6] M. Lohstroh, Í. Í. Romero, A. Goens, P. Derler, J. Castrillon, E. A. Lee, and A. Sangiovanni-Vincentelli, “Reactors: A deterministic model for composable reactive systems,” in *Cyber Physical Systems. Model-Based Design – Proceedings of the 9th Workshop on Design, Modeling and Evaluation of Cyber Physical Systems (CyPhy 2019) and the Workshop on Embedded and Cyber-Physical Systems Education (WESE 2019)*, R. Chamberlain, M. Edin Grimheden, and W. Taha, Eds. Cham: Springer International Publishing, Feb. 2020, pp. 59–85. [Online]. Available: https://link.springer.com/chapter/10.1007/978-3-030-41131-2_4
- [7] E. A. Lee and M. Lohstroh, *Generalizing Logical Execution Time*. Switzerland: Springer Nature, 2022, vol. LNCS 13660, pp. 1–22.
- [8] M. Lohstroh, C. Menard, A. Schulz-Rosengarten, M. Weber, J. Castrillon, and E. A. Lee, “A language for deterministic coordination across multiple timelines,” in *Forum for Specification and Design Languages (FDL)*. IEEE, September 15-17 2020, Conference Proceedings.
- [9] B. Sun, M. Theile, Z. Qin, D. Bernardini, D. Roy, A. Bastoni, and M. Caccamo, “Edge generation scheduling for dag tasks using deep reinforcement learning,” *IEEE Transactions on Computers*, vol. 73, no. 4, pp. 1034–1047, 2024.
- [10] J. Cardoso, C. Chanel, P. Chauvin, A. Hostallier, J. Lamaison, A. Mascarenas-Gonzales, E. Metral, and L. Alloza, “Lab on the real-time control of reaction wheel,” 2022, unpublished lab exercise for the course IMAE803: Real-time Control of Aerospace Systems, M.Sc in Aerospace Engineering, ISAE-SUPAERO.
- [11] Z. Manna and A. Pnueli, “Verifying hybrid systems,” in *Hybrid Systems*. Springer, 1993, pp. 4–35.
- [12] C. Hewitt, P. B. Bishop, and R. Steiger, “A universal modular ACTOR formalism for artificial intelligence,” in *Proceedings of the 3rd International Joint Conference on Artificial Intelligence. Stanford, CA, USA, August 20-23, 1973*, 1973, pp. 235–245.
- [13] J. B. Dennis, “First version data flow procedure language,” MIT Laboratory for Computer Science, Report MAC TM61, 1974.
- [14] W. A. Najjar, E. A. Lee, and G. R. Gao, “Advances in the dataflow computational model,” *Parallel Computing*, vol. 25, no. 13-14, pp. 1907–1929, December 1999.
- [15] G. Kahn, “The semantics of a simple language for parallel programming,” in *Proc. of the IFIP Congress 74*. North-Holland Publishing Co., 1974, Conference Proceedings, pp. 471–475.
- [16] T. A. Henzinger, B. Horowitz, and C. M. Kirsch, “Giotto: A time-triggered language for embedded programming,” in *EMSOFT 2001*, vol. LNCS 2211. Springer-Verlag, 2001, Conference Proceedings, pp. 166–184.
- [17] A. Benveniste and G. Berry, “The synchronous approach to reactive and real-time systems,” *Proceedings of the IEEE*, vol. 79, no. 9, pp. 1270–1282, 1991.

- [18] M. Verucchi, M. Theile, M. Caccamo, and M. Bertogna, "Latency-aware generation of single-rate DAGs from multi-rate task sets," in *IEEE Real-Time and Embedded Technology and Applications Symposium (RTAS)*, 2020, pp. 226–238.
- [19] S. Lin, Y. A. Manerkar, M. Lohstroh, E. Polgreen, S.-J. Yu, C. Jerad, E. A. Lee, and S. A. Seshia, "Towards building verifiable CPS using Lingua Franca," *ACM Trans. Embed. Comput. Syst.*, vol. 22, no. 5s, sep 2023. [Online]. Available: <https://doi.org/10.1145/3609134>
- [20] A. H. Ghamarian, M. C. Geilen, T. Basten, and S. Stuijk, "Throughput analysis of synchronous data flow graphs," *Proceedings - Design, Automation and Test in Europe, DATE*, pp. 116–121, 2006.
- [21] E. A. Lee and S. A. Seshia, *Introduction to Embedded Systems - A Cyber-Physical Systems Approach*, 2nd ed. Cambridge, MA, USA: MIT Press, 2017. [Online]. Available: <http://LeeSeshia.org>
- [22] A. Waterman, Y. Lee, D. Patterson, K. Asanovic, V. I. U. level Isa, A. Waterman, Y. Lee, and D. Patterson, "The risc-v instruction set manual," *Volume I: User-Level ISA, version*, vol. 2, 2014.
- [23] B. Lickly, I. Liu, S. Kim, H. D. Patel, S. A. Edwards, and E. A. Lee, "Predictable programming on a precision timed architecture," in *Proceedings of the 2008 International Conference on Compilers, Architectures and Synthesis for Embedded Systems*, ser. CASES '08. New York, NY, USA: Association for Computing Machinery, 2008, p. 137–146. [Online]. Available: <https://doi.org/10.1145/1450095.1450117>
- [24] M. Zimmer, D. Broman, C. Shaver, and E. A. Lee, "Flexpret: A processor platform for mixed-criticality systems," in *2014 IEEE 19th Real-Time and Embedded Technology and Applications Symposium (RTAS)*, 2014, pp. 101–110.
- [25] E. R. Jellum, S. Lin, P. Donovan, C. Jerad, E. Wang, M. Lohstroh, E. A. Lee, and M. Schoeberl, "Interpret: A time-predictable multicore processor," in *Proceedings of Cyber-Physical Systems and Internet of Things Week 2023*, ser. CPS-IoT Week '23. New York, NY, USA: Association for Computing Machinery, 2023, p. 331–336. [Online]. Available: <https://doi.org/10.1145/3576914.3587497>
- [26] C. Menard, M. Lohstroh, S. Bateni, M. Chorlian, A. Deng, P. Donovan, C. Fournier, S. Lin, F. Suchert, T. Tanneberger, H. Kim, J. Castrillon, and E. A. Lee, "High-performance deterministic concurrency using Lingua Franca," *ACM Trans. Archit. Code Optim.*, vol. 20, no. 4, oct 2023. [Online]. Available: <https://doi.org/10.1145/3617687>
- [27] S. M. Imam and V. Sarkar, "Savina - an actor benchmark suite: Enabling empirical evaluation of actor libraries," in *Proceedings of the 4th International Workshop on Programming Based on Actors Agents & Decentralized Control*, ser. AGERE! '14. New York, NY, USA: Association for Computing Machinery, 2014, p. 67–80. [Online]. Available: <https://doi.org/10.1145/2687357.2687368>
- [28] C. M. Kirsch and A. Sokolova, "The logical execution time paradigm," *Advances in Real-Time Systems*, pp. 103–120, 2012.
- [29] R. Ernst, L. Ahrendts, and K.-B. Gemmlau, "System level let: Mastering cause-effect chains in distributed systems," in *IECON 2018-44th Annual Conference of the IEEE Industrial Electronics Society*. IEEE, 2018, pp. 4084–4089.
- [30] J. Hui and S. A. Edwards, "The sparse synchronous model on real hardware," *ACM Transactions on Embedded Computing Systems*, 2022.
- [31] J. Hui, K. J. Edwards, and S. A. Edwards, "Timestamp peripherals for precise real-time programming," in *Proceedings of the 21st ACM-IEEE International Conference on Formal Methods and Models for System Design*, 2023, pp. 137–147.
- [32] R. L. Graham, "Bounds on multiprocessing timing anomalies," *SIAM Journal on Applied Mathematics*, vol. 17, no. 2, pp. 416–429, 1969.
- [33] Q. He, N. Guan, Z. Guo *et al.*, "Intra-task priority assignment in real-time scheduling of DAG tasks on multi-cores," *IEEE Transactions on Parallel and Distributed Systems*, vol. 30, no. 10, pp. 2283–2295, 2019.
- [34] S. Zhao, X. Dai, I. Bate, A. Burns, and W. Chang, "DAG scheduling and analysis on multiprocessor systems: Exploitation of parallelism and dependency," in *IEEE Real-Time Systems Symposium (RTSS)*, 2020, pp. 128–140.